Ab initio classical trajectories on the Born–Oppenheimer surface: Hessian-based integrators using fifth-order polynomial and rational function fits

John M. Millam, Vebjørn Bakken,[a] Wei Chen, William L. Hase, and H. Bernhard Schlegel[b]
Department of Chemistry, Wayne State University, Detroit, Michigan 48202

(Received 24 March 1999; accepted 24 May 1999)

Classical trajectories can be computed directly from electronic structure calculations without constructing a global potential-energy surface. When the potential energy and its derivatives are needed during the integration of the classical equations of motion, they are calculated by electronic structure methods. In the Born–Oppenheimer approach the wave function is converged rather than propagated to generate a more accurate potential-energy surface. If analytic second derivatives (Hessians) can be computed, steps of moderate size can be taken by integrating the equations of motion on a local quadratic approximation to the surface (a second-order algorithm). A more accurate integration method is described that uses a second-order predictor step on a local quadratic surface, followed by a corrector step on a better local surface fitted to the energies, gradients, and Hessians computed at the beginning and end points of the predictor step. The electronic structure work per step is the same as the second-order Hessian based integrator, since the energy, gradient and Hessian at the end of the step are used for the local quadratic surface for the next predictor step. A fifth-order polynomial fit performs somewhat better than a rational function fit. For both methods the step size can be a factor of 10 larger than for the second order approach without loss of accuracy.
© *1999 American Institute of Physics.* [S0021-9606(99)30131-8]

INTRODUCTION

Classical trajectory calculations[1] are a powerful tool for studying reaction dynamics and have been used widely. They provide much greater insight into the dynamics of reactions than variational transition state theory (VTST) and reaction path Hamiltonian methods.[2] Such calculations require accurate global potential-energy surfaces for the reaction systems. The traditional approach is to construct an analytical potential-energy function by fitting to experimental data and/or *ab initio* molecular-orbital calculations.[1] The classical equations of motion are then integrated numerically on the fitted surface, using well developed ordinary differential integration algorithms such as Runge–Kutta, predictor–corrector methods, etc.[3] The bottleneck in this procedure is the construction of the potential-energy surface.[4] Since there are no general methods for constructing accurate global potential-energy surfaces, each reaction must be treated as a special case, and it may take many months to build a suitable model surface for a specific reaction. Furthermore, the high dimensionality of most surfaces (i.e., $3N-6$ for nonlinear systems with N atoms) may necessitate the introduction of a number of assumptions and approximations, the validity of which may be difficult to test.

Because of advances in computer speed and improvements in molecular-orbital software, it has become possible to compute classical trajectories directly from electronic structure calculations without first fitting a global potential-energy surface (for a recent review see Ref. 5). In the Car–Parrinello method,[6] the electronic wave function is propagated along with the nuclei. In the Born–Oppenheimer approach, the wave function is converged to yield a more accurate potential-energy surface for the dynamics calculations. Classical trajectories can be calculated on this surface by using the analytical first derivatives (gradients) computed directly by the electronic structure method. If analytical second derivatives (Hessians) can be computed, significantly larger steps can be taken by calculating the classical equations of motion on a local quadratic approximation to the surface. In their pioneering work, Helgaker, Uggerud, and Jensen[7] used this approach to compute classical trajectories for the H_2+H reaction and for $CH_2OH^+ \rightarrow CHO^+ + H_2$ directly from the *ab initio* calculations. Local quadratic potential-energy surfaces were obtained from multiconfiguration self-consistent field (MCSCF) calculations of energies, gradients, and Hessians, as needed in the course of the integration. This alternative approach makes it possible to study the reaction dynamics of small molecules without fitting global analytical functions and introducing arbitrary assumptions. A growing number of systems have been studied by gradient-based and Hessian-based direct classical trajectory methods.[7–11]

The integration of classical trajectories using local quadratic surfaces requires modest step sizes because of the anharmonicity of the global molecular potential-energy surface. In this paper we present a more accurate Hessian based algorithm that involves a predictor step on a local quadratic

[a]Permanent address: Department of Chemistry, University of Oslo, P.O.B. 1033 Blindern, N-0315 Oslo, Norway.
[b]Electronic mail: hbs@chem.wayne.edu

 © 1999 American Institute of Physics

surface followed by a corrector step. The corrector step employs a fifth-order polynomial or a rational function fitted to the energy, gradient, and Hessian at the beginning and end points of each step. No additional *ab initio* calculations are required beyond those needed for the second-order method, since the energy, gradient, and Hessian calculated at the end of the current step are used for the local quadratic surface in the predictor phase of the next step. Test results indicate that the correction step allows an increase of a factor of ten or more in the step size. Our initial applications of this approach were to $H_2CO \rightarrow H_2+CO$,[9] $C_2H_4F \rightarrow H+C_2H_3F$,[10] and a model of retinal isomerization.[11]

METHODOLOGY

A local quadratic surface can be constructed from the analytical first and second derivatives of the energy calculated by molecular-orbital methods

$$V(\mathbf{x}) = E^0 + \mathbf{G}^{0t}(\mathbf{x}-\mathbf{x}^0) + \tfrac{1}{2}(\mathbf{x}-\mathbf{x}^0)^t\mathbf{H}^0(\mathbf{x}-\mathbf{x}^0), \tag{1}$$

where E^0, $\mathbf{G}^0$, and $\mathbf{H}^0$ are the energy, gradient, and Hessian evaluated at $\mathbf{x}^0$. Integration of the classical equations of motion is straightforward since the trajectory may be expressed in a closed analytical form. In Cartesian coordinates, Newton's equations of motion on the quadratic surface are

$$m_i d^2x_i/dt^2 = -dV(\mathbf{x})/dx_i = -G_i^0 - \Sigma_j H_{ij}^0(x_j - x_j^0). \tag{2}$$

Let $\mathbf{U}_i$ be the eigenvectors of the mass-weighted Hessian and h_i the corresponding eigenvalues, $\mathbf{U}_i^t(\mathbf{m}^{-1/2}\mathbf{H}\mathbf{m}^{-1/2})\mathbf{U}_j = h_i\delta_{ij}$, where $\mathbf{m}$ is a diagonal matrix of the atomic masses. In the instantaneous normal mode approach, the coordinates are transformed to the eigenvector space of the mass-weighted Hessian, and the equations of motion become

$$dp_i/dt = -g_i - h_i q_i, \tag{3}$$

where $q_i = \mathbf{U}_i^t\mathbf{m}^{1/2}(\mathbf{x}-\mathbf{x}^0)$, p_i is the conjugate momentum and $g_i = \mathbf{U}_i^t\mathbf{m}^{-1/2}\mathbf{G}$. It can be readily shown that the solutions to Eq. (3) are

$$\begin{aligned}
&q_i(t) = -a_i[1-\cos(\omega_i t)] + b_i\sin(\omega_i t), \quad h_i > 0,\\
&p_i(t) = \omega_i[-a_i\sin(\omega_i t) + b_i\cos(\omega_i t)],\\
&q_i(t) = -\tfrac{1}{2}g_i t^2 + p_i(0)t, \quad h_i = 0\\
&p_i(t) = p_i(0) - g_i t,\\
&q_i(t) = -a_i[1-\cosh(\omega_i t)] + b_i\sinh(\omega_i t), \quad h_i < 0,\\
&p_i(t) = \omega_i[-a_i\sinh(\omega_i t) + b_i\cosh(\omega_i t)],
\end{aligned} \tag{4}$$

where $a_i = g_i/h_i$, $b_i = p_i(0)/|\omega_i|$ and $\omega_i^2 = |h_i|$. The Cartesian coordinates and velocities are given by $\mathbf{x} = \mathbf{x}^0 + \mathbf{m}^{-1/2}\mathbf{U}\mathbf{q}$ and $d\mathbf{x}/dt = \mathbf{m}^{-1/2}\mathbf{U}\mathbf{p}$.

The quadratic approximation to the potential-energy surface is valid only for a given trust radius, τ. The time interval for the integration of the predictor step is adjusted so that the integration path length is equal to the trust radius. This forms the basic step of the second order Hessian-based trajectory integration method.[7] The energy, gradient, and Hessian are then calculated again, and the integration of the equations of motion is repeated for the next step.

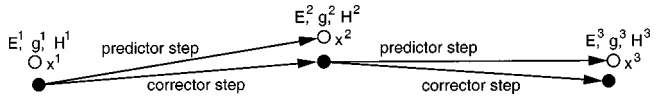

FIG. 1. Hessian-based predictor–corrector algorithm for integration of trajectories. A quadratic approximation to the surface at $\mathbf{x}^1$ is used in a predictor step to obtain $\mathbf{x}^2$; the energies, gradients, and Hessians at $\mathbf{x}^1$ and $\mathbf{x}^2$ are fitted by a fifth-order polynomial or rational function; a correction step is then taken on this fitted surface; the procedure is repeated for the next step, starting with the quadratic approximation to the surface at $\mathbf{x}^2$.

A more accurate method can be constructed by starting with the second-order method as a predictor step, and followed by a corrector step. This sequence is outlined in Fig. 1. At the end of the predictor step, the energy, gradient, and Hessian are recalculated. A better local approximation to the potential-energy surface is obtained by fitting a higher-order surface to the energy, gradient, and Hessian at the beginning and at the end of the predictor step. Standard numerical methods can then be used to integrate the trajectory on this fitted surface. In the present implementation, the Bulirsch–Stoer method is used with the thresholds set so that the error in the integration is less than 10^{-6} amu$^{1/2}$ bohr and the error in the energy is less than 10^{-10} hartree. This trajectory is integrated for the same time interval as used for the predictor step. The Hessian at the end of the current predictor step is used to calculate the next predictor step. Thus, like the second-order method, only one Hessian is calculated per step. However, the more accurate local fitted surface allows larger steps to be taken.

Two types of local fitted surfaces have been examined—a fifth-order polynomial, and a rational function fit. To carry out the fit, the Cartesian coordinates are rotated so that one component is parallel to the predictor step, $x_\parallel$, and the others are perpendicular to the step, $\mathbf{x}_\perp$. For given displacements parallel and perpendicular to the path, $\Delta x_\parallel$ and $\Delta\mathbf{x}_\perp$, the energies, first and second derivatives parallel to the path are given by

$$\begin{aligned}
&E^a = E^1 + \mathbf{g}^1{}_\perp{}^t\Delta\mathbf{x}_\perp + \tfrac{1}{2}\Delta\mathbf{x}_\perp{}^t\mathbf{H}^1{}_{\perp,\perp}\Delta\mathbf{x}_\perp,\\
&g^a = g^1{}_\parallel + \mathbf{H}^1{}_{\parallel,\perp}\Delta\mathbf{x}_\perp, \quad h^a = H^1{}_{\parallel,\parallel},\\
&E^b = E^2 + \mathbf{g}^2{}_\perp{}^t\Delta\mathbf{x}_\perp + \tfrac{1}{2}\Delta\mathbf{x}_\perp{}^t\mathbf{H}^2{}_{\perp,\perp}\Delta\mathbf{x}_\perp,\\
&g^b = g^2{}_\parallel + \mathbf{H}^2{}_{\parallel,\perp}\Delta\mathbf{x}_\perp, \quad h^b = \mathbf{H}^2{}_{\parallel,\parallel},
\end{aligned} \tag{5}$$

where E^1, $\mathbf{g}^1$, and $\mathbf{H}^1$ are calculated at the beginning of the predictor step, $\mathbf{x}^1$, and E^2, $\mathbf{g}^2$, and $\mathbf{H}^2$ at the end of the predictor step, $\mathbf{x}^2$.

A good approximation to the potential-energy surface can be constructed by fitting a fifth order polynomial to E^a, g^a, h^a, E^b, g^b, and h^b.

$$\begin{aligned}
V(\mathbf{x}) = {} & E^a(\Delta\mathbf{x}_\perp)y_1(\Delta\mathbf{x}_\parallel) + g^a(\Delta\mathbf{x}_\perp)y_2(\Delta\mathbf{x}_\parallel)\\
& + h^a(\Delta\mathbf{x}_\perp)y_3(\Delta x_\parallel) + E^b(\Delta\mathbf{x}_\perp)y_4(\Delta x_\parallel)\\
& + g^b(\Delta\mathbf{x}_\perp)y_5(\Delta x_\parallel) + h^b(\Delta\mathbf{x}_\perp)y_6(\Delta x_\parallel).
\end{aligned} \tag{6}$$

The y's are the appropriate fifth-order interpolating polynomials listed in the Appendix.

Alternatively, a rational function approximation to the surface can be obtained by fitting a quartic polynomial divided by a quadratic polynomial to E^a, g^a, h^a, E^b, g^b, and h^b.

$$V(\mathbf{x}) = \frac{p_0(\Delta\mathbf{x}_\perp) + p_1(\Delta\mathbf{x}_\perp)\Delta x_\parallel + p_2(\Delta\mathbf{x}_\perp)\Delta x_\parallel^2 + p_3(\Delta\mathbf{x}_\perp)\Delta x_\parallel^3 + p_4(\Delta\mathbf{x}_\perp)\Delta x_\parallel^4}{1 + q_1(\Delta\mathbf{x}_\perp)\Delta x_\parallel + q_2(\Delta\mathbf{x}_\perp)\Delta x_\parallel^2}. \tag{7}$$

The determination of the p's and q's is described in the Appendix.

If Cartesian coordinates are used for the fitted surface, the local potential-energy surface is not invariant to overall rotation. Residual problems with numerical noise and with translational and rotational invariance can be removed by projecting the mass-weighted gradient, **Pg**. The appropriate projector is given by

$$\mathbf{P} = \mathbf{I} - \sum_{i=1}^{6} \mathbf{U}_i \mathbf{U}_i^t, \tag{8}$$

where $\mathbf{U}_1 - \mathbf{U}_6$ are the normalized vectors corresponding to overall translation and rotation in mass weighted coordinates. An alternate solution is to use internal coordinates for the surface fitting to ensure translational and rotational invariance. This will be explored in a subsequent paper.

NUMERICAL TESTS

The $H_2CO \rightarrow H_2 + CO$ reaction has been used to examine the behavior of the Hessian based integration schemes. The reaction involves only a small number of atoms and, when started from the transition state, trajectories reach the product region in ~35 fs. Thus numerous tests can be carried out without excessive computational effort. The system contains a mixture of high- and low-frequency modes and the products are rotationally and vibrationally excited; hence it should provide a reasonable test for various aspects of the trajectory calculations. The electronic structure calculations were carried out at the RHF/3-21G (restricted Hartree–Fock) level of theory with the current development version of the GAUSSIAN series of programs.[12] As in the previous paper,[9] the trajectories at 0 K were started at the transition state with 5.145 kcal/mol translational energy along the transition vector, zero-point energy in the other vibrational modes and no rotational energy. For the trajectories at 298 K, the transition structure was given $\frac{1}{2}$ kT rotational energy about each principle axis, but only zero-point energy for the vibrations.

Figure 2 compares different step sizes in the integration of a trajectory. The H–H bond length should be the most sensitive indicator because H_2 has a high-vibrational frequency and is produced vibrationally excited. All of the trajectories from 0.005 to 0.320 amu$^{1/2}$ bohr are superimposible (for clarity only the points for 0.320 amu$^{1/2}$ bohr are marked explicitly). Trajectories with a step size of 0.480 amu$^{1/2}$ bohr starts to deviate slightly, and with a step size of 0.640 amu$^{1/2}$ bohr they differ significantly. Increasing the rotational temperature to 298 K does not change this picture. The C–O bond length is even less sensitive to the size of the steps. At a step size of 0.320 amu$^{1/2}$ bohr, 50–55 steps are required for the 30–35 fs needed to reach the products.

The conservation of the total energy as a function of step size is shown in Fig. 3 in atomic units. The accumulated error in the energy is the sum of the absolute values of the changes in the total energy for each step. The final error in the total energy is about an order of magnitude lower than the accumulated error. The energy difference between the transition state and the products at this level of theory is 0.166 hartree or 104 kcal/mol and energy is conserved to 10^{-4}–10^{-8} hartree depending on the step size and the angular momentum. At 0 K, the fifth-order polynomial fit performs significantly better than the rational function fit. At 298 K the difference between the fifth order and rational function methods is much less pronounced, but both integra-

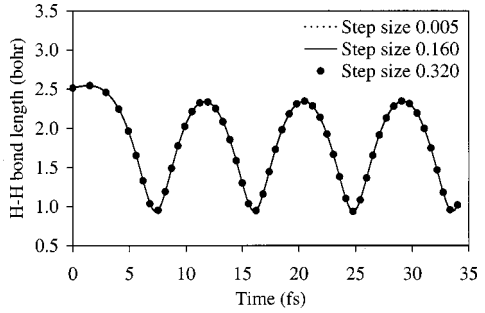

FIG. 2. Comparison of changes in the H–H bond length for trajectories of $H_2CO \rightarrow H_2 + CO$ starting at the transition state. For the step sizes indicated, all of the trajectories are superimposable; points on the trajectory are marked only for the largest step size.

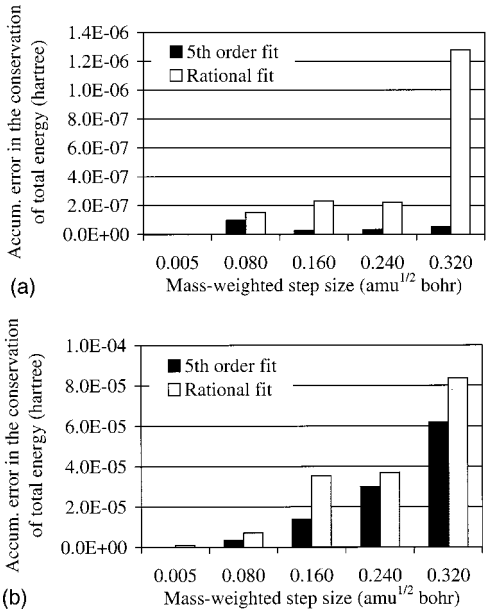

FIG. 3. Accumulated error in the conservation of energy as a function of step size for trajectories at 0 and 298 K.

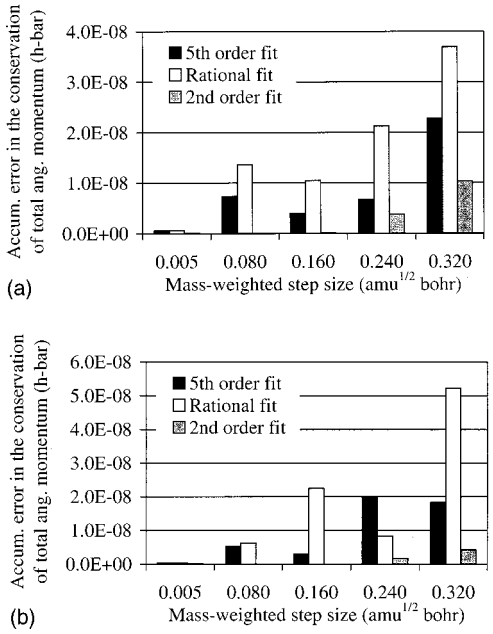

FIG. 4. Accumulated error in the conservation of angular momentum as a function of step size for trajectories at 0 and 298 K.

tors have errors that are one to two orders of magnitude larger than at 0 K. The second-order method is not shown on these plots, because the errors in the conservation of the total energy are three to four orders of magnitude larger than the fifth-order fit for step sizes up to 0.320 $\text{amu}^{1/2}$ bohr.

The conservation of total angular momentum as a function of step size is shown in Fig. 4 in units of $\hbar$. At 298 K the total angular momentum is $\sim 14\ \hbar$. Projection reduces the error in the conservation of angular momentum by ~ 8 orders of magnitude. The behavior with different step sizes is very similar at both temperatures. As was found for the energy, the rational function fit is somewhat inferior to the fifth-order polynomial fit. Surprisingly, the second-order method with projection conserves total angular momentum somewhat better than either of the fifth order or the rational polynomial fits.

The order of a numerical differential equation integration scheme can be obtained by determining the average error as a function of the step size. Figure 5 is a log–log plot of the average of the absolute value of the change in the total energy per step (i.e., the accumulated error divided by the number of steps) as a function of the step size at 298 K. Although the energy conservation is better at 0 K, the plots of the errors as a function of step size are somewhat more erratic. The quadratic and the fifth-order fits yield slopes of ~ 3, indicating they are both second-order methods with respect to the step size. The fifth-order polynomial fit has a much smaller error as a result of the better fit to the potential-energy surface parallel to the step. However, perpendicular to the step, this fit is only quadratic. Thus it is the error in the component of the trajectory perpendicular to the overall step that determines the order of the integrator using the fifth-order fit.

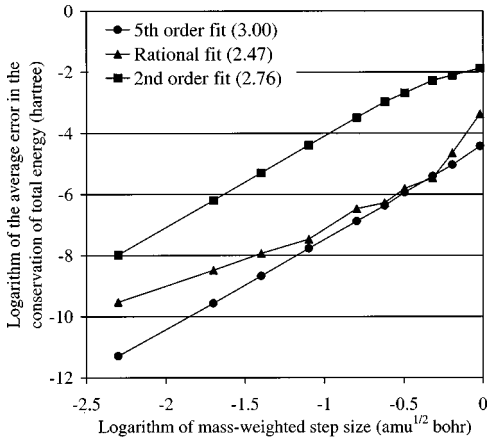

FIG. 5. A log–log plot of the average error in the conservation of energy as a function of the step size at 298 K. The slopes of the lines fitted to each set of points are indicated in parentheses.

CONCLUSIONS

For a given step size, the fifth-order and rational function fits significantly reduce the error relative to a simple quadratic function. As can be seen from Fig. 5, the error in the total energy is three orders of magnitude lower with essentially no increase in computational cost. The fifth-order fit is generally somewhat better than the rational function fit, and step sizes of up to 0.320 $\text{amu}^{1/2}$ bohr can be used with very good conservation of the total energy and angular momentum. With comparable conservation of the energy, integration using the fifth-order polynomial is an order of magnitude faster than the simple quadratic fit for the test cases considered in the present work.

ACKNOWLEDGMENTS

This research was supported by a grant from the National Science Foundation (CHE 9400678 and CHE 9974005) and by Gaussian, Inc. V.B. would like to thank the Research Council of Norway for a travel grant in support of this work.

APPENDIX

Fifth-order polynomial fit

The interpolating polynomials for fitting the surface are

$$
\begin{aligned}
y_1(u) &= 1 - 10u^3 + 15u^4 - 6u^5, \\
y_2(u) &= s(u - 6u^3 + 8u^4 - 3u^5), \\
y_3(u) &= s^2/2\,(u^2 - 3u^3 + 3u^4 - u^5), \\
y_4(u) &= 10u^3 - 15u^4 + 6u^5, \\
y_5(u) &= s(-4u^3 + 7u^4 - u^5), \\
y_6(u) &= s^2/2\,(u^3 - 2u^4 + u^5),
\end{aligned}
\tag{A1}
$$

where $u = \Delta x_{\parallel}/s$ and $s = |\mathbf{x}^2 - \mathbf{x}^1|$.

Rational polynomial fit

The determination of the coefficients for the rational polynomial approximation is a bit more involved.

$$V(x)=\frac{p_0+p_1\Delta x+p_2\Delta x^2+p_3\Delta x^3+p_4\Delta x^4}{1+q_1\Delta x+q_2\Delta x^2}. \tag{A2}$$

For a given perpendicular displacement, the energy, gradient, and Hessian at the beginning of the step ($\Delta x=0$) and the end of the step ($\Delta x=s$) are E^a, g^a, h^a, and E^b, g^b, h^b, respectively, calculated by Eq. (5). Since there are seven unknowns and only six pieces of data, an additional constraint is needed. Coefficients p_0, p_1, and p_2 can be obtained readily by fitting $V(x)$ to E^a, g^a and h^a at $\Delta x=0$.

$$p_0=E^a,\quad p_1=E^aq_1+g^a,\quad p_2=E^aq_2+g^aq_1+1/2h^a. \tag{A3}$$

Fitting $V(x)$ to E^b, g^b, and h^b at $\Delta x=s$ leads to three linear equations with four unknowns (p_3, p_4, q_1, and q_2). To simplify the equations, all the q_1 dependence is put on the right-hand-side of the equation

$$\begin{aligned}
&\mathbf{Cr}=\mathbf{F}q_1+\mathbf{D},\\
&r_1=q_2,\quad r_2=p_3,\quad r_3=p_4,\\
&F_1=s(E^b-E^a)-s^2g^a,\\
&F_2=(E^b-E^a)+s(g^b-2g^a),\\
&F_3=2(g^b-g^a)+sh^b,\\
&D_1=(E^b-E^a)-sg^a-\tfrac{1}{2}s^2h^a,\\
&D_2=(g^b-g^a)-sh^a,\quad D_3=(h^b-h^a),\\
&C_{11}=s^2(E^a-E^b),\quad C_{12}=s^3,\quad C_{13}=s^4,\\
&C_{21}=2s(E^a-E^b)-s^2g^b,\quad C_{22}=3s^2,\quad C_{23}=4s^3,\\
&C_{31}=2(E^a-E^b)-4sg^b-s^2h^b,\quad C_{32}=6s,\quad C_{33}=12s^2.
\end{aligned} \tag{A4}$$

The solution to these equations depends on q_1:

$$\mathbf{r}=\mathbf{C}^{-1}\mathbf{F}q_1+\mathbf{C}^{-1}\mathbf{D}=\mathbf{A}q_1+\mathbf{B}. \tag{A5}$$

When the denominator of the rational function goes to zero, there are singularities at $\Delta x_s=(-q_1\pm(q_1{}^2-4q_2)^{1/2})/2q_2$. These singularities can be moved away from the interpolating regions by constraining q_1 such that the discriminant is as negative as possible.

$$(q_1^2-4q_2)=\phi. \tag{A6}$$

By combining this with Eq. (A5) for q_2 (i.e., $q_2=A_1q_1+B_1$), we get

$$\begin{aligned}
&q_1=2A_1\pm(4A_1^2+4B_1+\phi)^{1/2},\\
&q_2=2A_1^2+B_1\pm A_1(4A_1^2+4B_1+\phi)^{1/2}.
\end{aligned} \tag{A7}$$

To have real coefficients, $(4A_1^2+4B_1+\phi)$ must be greater than zero. Thus, we cannot choose ϕ arbitrarily; however, $\phi=-4A_1^2-4B_1$ is a unique and optimal choice, leading to

$$q_1=2A_1,\quad q_2=2A_1^2+B_1. \tag{A8}$$

Specific values for p_3 and p_4 can then be obtained from Eq. (A5), p_0, p_1, and p_2 can be obtained from Eqs. (A3).

For the integration of the equations of motion, we also need the gradient of the fitted potential. For the fifth-order polynomial surface, the derivatives of the interpolating polynomials are required. For the rational function fit, the coefficients depend on the perpendicular displacement. The derivatives of the coefficients are obtained by solving the derivative of Eqs. (A4).

[1] D. L. Bunker, Methods Comput. Phys. **10**, 287 (1971); L. M. Raff and D. L. Thompson, in *Theory of Chemical Reaction Dynamics*, edited by M. Baer (CRC, Boca Raton, 1985); *Advances in Classical Trajectory Methods*, edited by W. L. Hase (JAI, Stamford, 1991), Vols. 1–3; D. L. Thompson, in *Encyclopedia of Computational Chemistry*, edited by P. v. R. Schleyer, N. L. Allinger, T. Clark, J. Gasteiger, P. A. Kollman, H. F. Schaefer III, and P. R. Schreiner (Wiley, Chichester, 1998), p. 3056, and references therein.

[2] D. G. Truhlar, B. C. Garrett, and S. J. Klippenstein, J. Phys. Chem. **100**, 12771 (1996), and references therein; D. G. Truhlar and B. C. Garrett, Acc. Chem. Res. **13**, 440 (1980); W. H. Miller, N. C. Handy, and J. E. Adams, J. Chem. Phys. **72**, 99 (1980); E. Kraka, in *Encyclopedia of Computational Chemistry*, edited by P. v. R. Schleyer, N. L. Allinger, T. Clark, J. Gasteiger, P. A. Kollman, H. F. Schaefer III, and P. R. Schreiner (Wiley, Chichester, 1998), p. 2437, and references therein.

[3] C. W. Gear, *Numerical Initial Value Problems in Ordinary Differential Equations* (Prentice-Hall, Englewood Cliffs, 1971); J. Stoer and R. Bulirsch, *Introduction to Numerical Analysis* (Springer, New York, 1980); W. H. Press, B. P. Flannery, S. A. Teukolsky, and W. T. Vetterlin, *Numerical Recipes* (Cambridge University Press, Cambridge, 1989).

[4] G. C. Schatz, Rev. Mod. Phys. **61**, 669 (1989); G. C. Schatz, in *Advances in Molecular Electronic Structure Theory*, edited by T. H. Dunning (JAI, London, 1990).

[5] For a recent review of *ab initio* classical trajectory methods and a comparison of Born–Oppenheimer and Car–Parrinello methods see K. Bolton, W. L. Hase, and G. H. Peshlherbe, in *Modern Methods for Multidimensional Dynamics Computation in Chemistry*, edited by D. L. Thompson (World Scientific, Singapore, 1998), p. 143.

[6] R. Car and M. Parrinello, Phys. Rev. Lett. **55**, 2471 (1985); M. E. Tuckerman, P. J. Ungar, T. von Rosenvinge, and M. L. Klein, J. Phys. Chem. **100**, 12878 (1996), and references therein.

[7] T. Helgaker, E. Uggerud, and H. J. A. Jensen, Chem. Phys. Lett. **173**, 145 (1990); E. Uggerud and T. Helgaker, J. Am. Chem. Soc. **114**, 4265 (1992); H.-H. Bueker, T. Helgaker, K. Ruud, and E. Uggerud, J. Phys. Chem. **100**, 15388 (1996); H.-H. Bueker and E. Uggerud, *ibid.* **99**, 5945 (1995); K. Ruud, T. Helgaker, and E. Uggerud, J. Mol. Struct.: THEOCHEM **393**, 59 (1997); E. L. Oiestad and E. Uggerud, Int. J. Mass Spectrom. Ion Phys. **165**, 39 (1997).

[8] For some additional examples of Born–Oppenheimer trajectory applications, see E. A. Carter, Chem. Phys. Lett. **240**, 261 (1995); Z. H. Liu, L. E. Carter, and E. A. Carter, J. Phys. Chem. **99**, 4355 (1995); R. W. Warren and B. I. Dunlap, Phys. Rev. A **57**, 899 (1998); T. Takayanagi and A. Yokoyama, Bull. Chem. Soc. Jpn. **68**, 2245 (1995); K. C. Thompson, M. J. T. Jordan, and M. A. Collins, J. Chem. Phys. **108**, 564 (1998); Y. M. Rhee, T. G. Lee, S. C. Park *et al.*, J. Chem. Phys. **106**, 1003 (1997); M. J. T. Jordan, K. C. Thompson, and M. A. Collins, J. Chem. Phys. **102**, 5647 (1995); D. A. Gibson, I. V. Ionova, S. Clifford, M. J. Bearpark, F. Bernardi *et al.*, J. Am. Chem. Soc. **118**, 7353 (1996); M. J. Bearpark, F. Bernardi, M. Olivucci *et al.*, *ibid.* **118**, 5254 (1996); M. J. Bearpark, F. Bernardi, S. Clifford *et al.*, *ibid.* **118**, 169 (1996); G. H. Peslherbe and W. L. Hase, Chem. Phys. **104**, 7882 (1996); G. H. Peslherbe, H. B. Wang, and W. L. Hase, J. Am. Chem. Soc. **118**, 2257 (1996); C. Doubleday, K. Bolton, G. H. Peslherbe *et al.*, *ibid.* **118**, 9922 (1996); K. Bolton, W. L. Hase, and C. Doubleday, Ber. Bunsenges. Phys. Chem. **101**, 414 (1997); H. Tachikawa and M. Igarashi, J. Phys. Chem. **102**, 8648 (1998), and references therein; M. Igarashi and H. Tachikawa, Int. J. Mass Spectrom. Ion Phys. **181**, 151 (1998); for early examples see I. S. Y. Wang and M. Karplus, J. Am. Chem. Soc. **95**, 8160 (1973); C. Leforestier, J. Chem. Phys. **68**, 4406 (1978).

[9] W. Chen, W. L. Hase, and H. B. Schlegel, Chem. Phys. Lett. **228**, 436 (1994).

[10] K. Bolton, K. W. L. Hase, H. B. Schlegel, and K. Song, Phys. Chem. Chem. Phys. **1**, 999 (1999).

[11] T. Vreven, F. Bernardi, M. Garavelli, M. Olivucci, M. A. Robb, and H. B. Schlegel, J. Am. Chem. Soc. **119**, 12687 (1997).
[12] GAUSSIAN 98, M. J. Frisch, G. W. Trucks, H. B. Schlegel, G. E. Scuseria, M. A. Robb, J. R. Cheeseman, V. G. Zakrzewski, J. A. Montgomery, Jr., R. E. Stratmann, J. C. Burant, S. Dapprich, J. M. Millam, A. D. Daniels, K. N. Kudin, M. C. Strain, O. Farkas, J. Tomasi, V. Barone, M. Cossi, R. Cammi, B. Mennucci, C. Pomelli, C. Adamo, S. Clifford, J. Ochterski, G. A. Petersson, P. Y. Ayala, Q. Cui, K. Morokuma, D. K. Malick, A. D. Rabuck, K. Raghavachari, J. B. Foresman, J. Cioslowski, J. V. Ortiz, B. B. Stefanov, G. Liu, A. Liashenko, P. Piskorz, I. Komaromi, R. Gomperts, R. L. Martin, D. J. Fox, T. Keith, M. A. Al-Laham, C. Y. Peng, A. Nanayakkara, C. Gonzalez, M. Challacombe, P. M. W. Gill, B. Johnson, W. Chen, M. W. Wong, J. L. Andres, C. Gonzalez, M. Head-Gordon, E. S. Replogle, and J. A. Pople (Gaussian, Inc., Pittsburgh, PA, 1998).